Electronic Supplementary Information for:

Intersystem Crossing via Charge Recombination in a Perylene-Naphthalimide Compact Electron Donor/Acceptor Dyad

Muhammad Imran,[a]‡ Ahmed M. El-Zohry,[b]‡ Clemens Matt,[c]‡ Maria Taddei,[d] Sandra Doria,[d] Laura Bussotti,[d] Paolo Foggi,[d,f] Jianzhang Zhao,[a,] Mariangela Di Donato,[d,e,]* Omar F. Mohammed[b,]* and Stefan Weber [c,]**

[a] State Key Laboratory of Fine Chemicals, School of Chemical Engineering, Dalian University of Technology, 2 Ling Gong Rd., Dalian 116024, China. E-mail: zhaojzh@dlut.edu.cn

[b] KAUST Solar Center, Division of Physical Sciences and Engineering, King Abdullah University of Science and Technology (KAUST), Thuwal 23955-6900, Kingdom of Saudi Arabia. E-mail: omar.abdelsaboor@kaust.edu.sa

[c] Institute of Physical Chemistry, Albert-Ludwigs-Universität Freiburg, Albertstr. 21, 79104 Freiburg, Germany. E-mail: stefan.weber@physchem.uni-freiburg.de

[d] LENS (European Laboratory for Non-Linear Spectroscopy), via N. Carrara 1, 50019 Sesto Fiorentino, FI, Italy

[e] ICCOM-CNR, via Madonna del Piano 10, I-50019 Sesto Fiorentino (FI), Italy

E-mail: didonato@lens.unifi.it

[f] Dipartimento di Chimica, Università di Perugia, via Elce di Sotto 8, I-06123 Perugia, Italy

‡ M. I., A. M. E. and C. M. contributed equally to this work.

Index

1. Synthesis of the compounds

Synthesis of compound 2. Compound **2** was synthesized following a similar method as we reported previously.[1] Under N_2 atmosphere, a solution of compound **1** (perylene. 1.0 g, 3.96 mmol) in DMF (20 mL) was stirred at room temperature. After that, *N*-bromosuccinimide (NBS. 693 mg, 3.96 mmol) in (20 mL) DMF solution was added dropwise into the reaction mixture within 30 minutes. The mixture was stirred overnight. On completion of reaction, water (50 mL) was added to give yellow solid, which was collected by filtration. The crude solid is 3-bromoperylene (1.10 g, yield: 84%). This compound was directly used for the next reaction without further purification. Only few mg was purified for some spectral measurements by column chromatography (silica gel, DCM/ PE = 1:4, v/v). TOF MS EI$^+$: Calcd ($[C_{20}H_{11}Br]^+$), *m/z* = 330.0044; found, *m/z* = 330.0039.

Synthesis of compound 3. Compound **3** was synthesized following a reported method.[2] Under N_2 atmosphere, compound **2** (496.8 mg, 1.5 mmol), bis(pinacolato)diboron (571.3 mg, 2.25 mmol) and potassium acetate (442.0 mg, 4.5 mmol) were mixed in dry 1,4-dioxane (75 mL). Purged the reaction mixture with N_2 for 30 minutes and $Pd(dppf)Cl_2{\cdot}CH_2Cl_2$ (45.0 mg, 0.05 mmol) was added. Allowed the reaction mixture to stirred at 80 °C for 19 h. On completion the organic layer was extracted with DCM (4 × 50 mL) by washing with brine and dried over anhydrous Na_2SO_4. Solvent was removed under reduced pressure and crude product was purified by column chromatography (silica gel, DCM/ PE = 1:2, v/v) to give yellowish orange solid (350 mg, yield: 62%). Mp: 233.0 – 234.0 °C. ^{1}H NMR ($CDCl_3$, 400 MHz): δ = 8.67 (d, 2H, *J* = 8.0 Hz), 8.25 – 8.17 (m, 4H), 8.08 (d, 1H, *J* = 8.0 Hz), 7.71 – 7.66 (m, 2H),

7.56 – 7.46 (m, 3H), 1.45 (s, 12H). TOF MS EI+: Calcd ([$C_{26}H_{23}BO_2$] +), *m/z* = 378.1791; found, *m/z* = 378.1783.

Synthesis of compound 4. Compound **4** was synthesized following a modified method.[3] Under N_2 atmosphere, 4-bromo-1,8-naphthalic anhydride (831.0 mg, 3.0 mmol) and *n*-butylamine (219.0 mg, 3.0 mmol) were mixed in ethanol (30 mL). The reaction mixture was refluxed for 8 h. After that, the reaction mixture was cooled to room temperature and solvent was removed under reduced pressure. Crude product was purified by column chromatography (silica gel, DCM/ PE = 2:1, v/v) to give white solid (500 mg, yield: 51%). ^{1}H NMR ($CDCl_3$, 400 MHz): δ = 8.65 (d, 1H, *J* = 8.0 Hz), 8.56 (d, 1H, *J* = 8.0 Hz), 8.41 (d, 1H, *J* = 8.0 Hz), 8.04 (d, 1H, *J* = 8.0 Hz), 7.85 – 7.82 (m, 1H), 4.17 (t, 2H, *J* = 8.0 Hz), 1.75 – 1.68 (m, 2H), 1.48 – 1.42 (m, 2H), 0.98 (t, 3H, *J* = 8.0 Hz). TOF MS EI+: Calcd ([$C_{16}H_{14}BrNO_2$] +), *m/z* = 331.0208; found, *m/z* = 331.0213.

Synthesis of compound NI-Ph. Under N_2 atmosphere, compound **4** (265.7 mg, 0.8 mmol), phenylboronic acid (97.5 mg, 0.8 mmol), K_2CO_3 (330 mg, 2.3 mmol) and EtOH/toluene/H_2O (v/v/v = 2: 2:1, 50 mL) were mixed together. After purged with N_2 for 15 minutes, $Pd(PPh_3)_4$ (20.2 mg, 0.039 mmol) was added and refluxed at 80 °C for 8 h. After completion of the reaction, the mixture was cooled to room temperature and extracted with DCM (4 × 50 mL). The organic layer was washed with H_2O and dried over anhydrous Na_2SO_4. Solvent was removed under reduced pressure and crude product was purified by column chromatography (silica gel, DCM/*n*-hexane = 1:3, v/v) to give white solid (150 mg, yield: 57%). Mp: 147.0 – 148.0 °C. ^{1}H NMR ($CDCl_3$, 400 MHz): δ = 8.66 (d, 2H, *J* = 8.0 Hz), 8.29 (d, 1H, *J* = 8.0 Hz), 7.72 (d, 2H), 7.60 – 7.52 (m, 5H), 4.26 (t, 2H, *J* = 8.0 Hz), 1.81 – 1.73 (m, 2H),

1.54 – 1.45 (m, 2H), 1.02 (t, 3H, *J* = 8.0 Hz). ^{13}C NMR ($CDCl_3$, 125 MHz): δ 164.32, 164.12, 146.82, 138.86, 132.56, 131.12, 130.77, 130.07, 129.87, 128.65, 128.46, 127.82, 126.80, 122.96, 121.85, 40.28, 30.25, 20.42, 13.86. TOF MS EI$^+$: Calcd ($[C_{22}H_{19}NO_2]^+$), *m/z* = 329.1416; found, *m/z* = 329.1420.

Synthesis of compound Pery-Ph. This compound was synthesized following a modified method.[4] Under N_2 atmosphere, 3-bromoperylene (460, mg, 4.2 mmol), and phenylboronic acid (170.8 mg, 1.4 mmol), K_2CO_3 (580.0 mg, 4.2 mmol, and EtOH/toluene/H_2O (v/v/v = 2:2:1, 100 mL) were mixed together. After purged with N_2 for 20 minutes, $Pd(PPh_3)_4$ (80.8 mg, 0.07 mmol, 5 mol %) was added and refluxed at 80 °C for 8 h. On completion of the reaction, the reaction mixture cooled to room temperature and extracted with DCM (4 × 50 mL) and the combined organic layers were dried over anhydrous $NaSO_4$. Solvent was removed under reduced pressure and crude product was purified by column chromatography (silica gel, DCM/*n*-hexane = 1:10, v/v) to give yellow solid (328.2 mg, yield: 72%). Mp: 199–200 °C. ^{1}H NMR ($CDCl_3$, 400 MHz): δ = 8.27 – 8.22 (m, 4H, *J*), 7.78 (d, 1H, *J* = 8.0 Hz), 7.72 (d, 2H, *J* = 8.0 Hz), 7.55 – 7.50 (m, 6H), 7.47 – 7.43 (m, 3H). TOF MS EI$^+$: Calcd ($[C_{26}H_{16}]^+$), *m/z* = 328.1252; found, *m/z* = 328.1257.

2. Molecular structural characterization data (NMR and MS spectra)

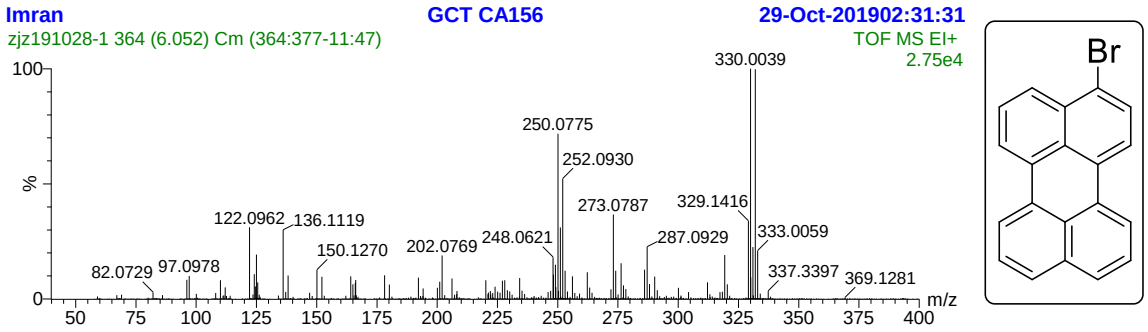

Fig. S1 TOF-MS EI⁺ spectrum of compound **2**.

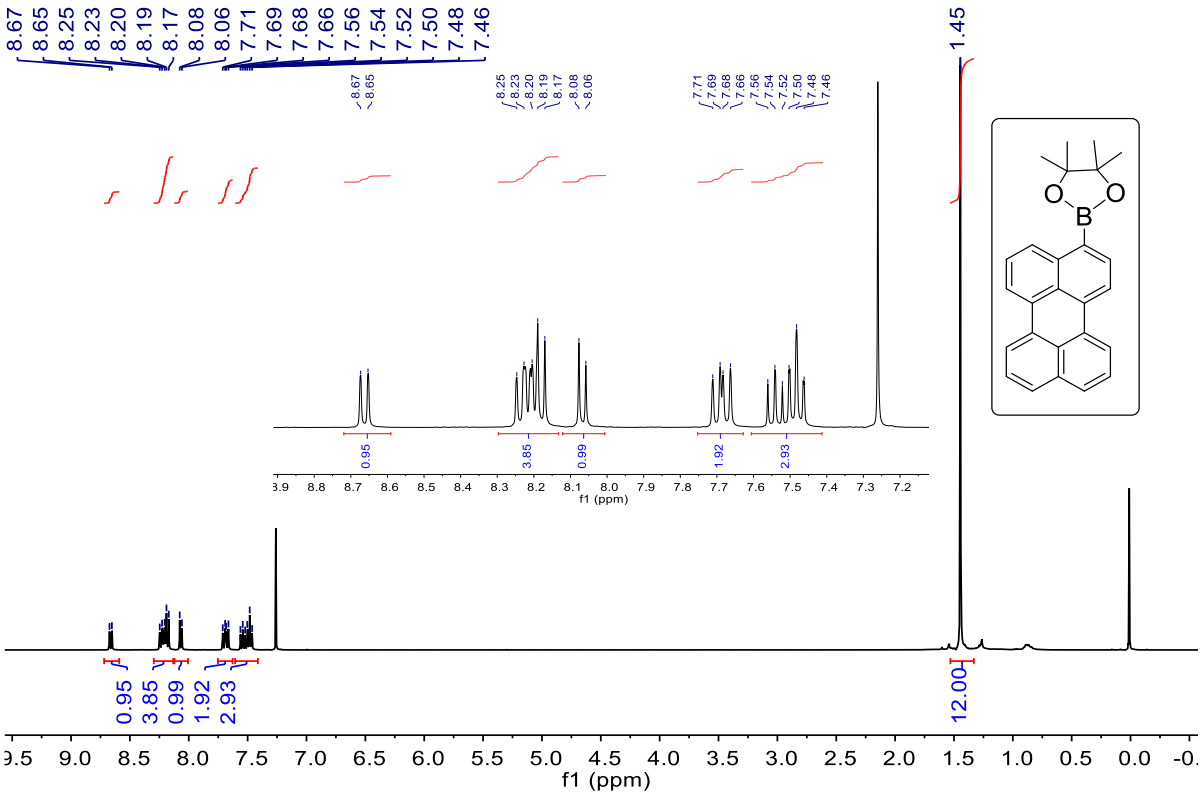

Fig. S2 ^{1}H NMR spectrum of compound **3** in $CDCl_3$ (400 MHz), 25 °C.

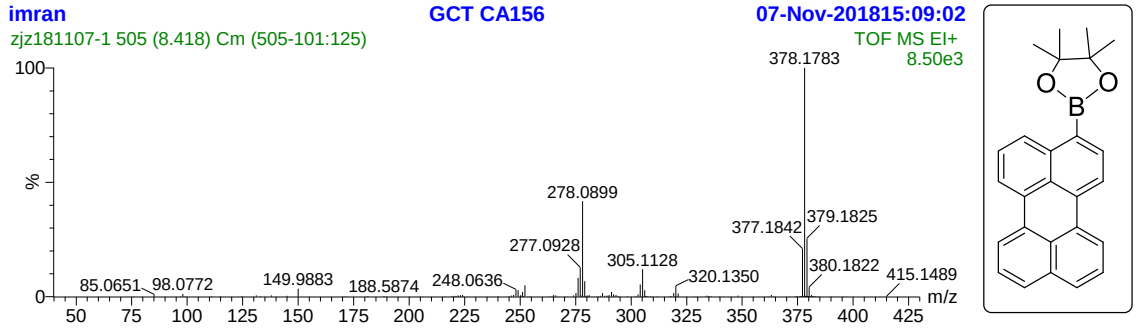

Fig. S3 TOF-MS EI⁺ spectrum of compound **3**.

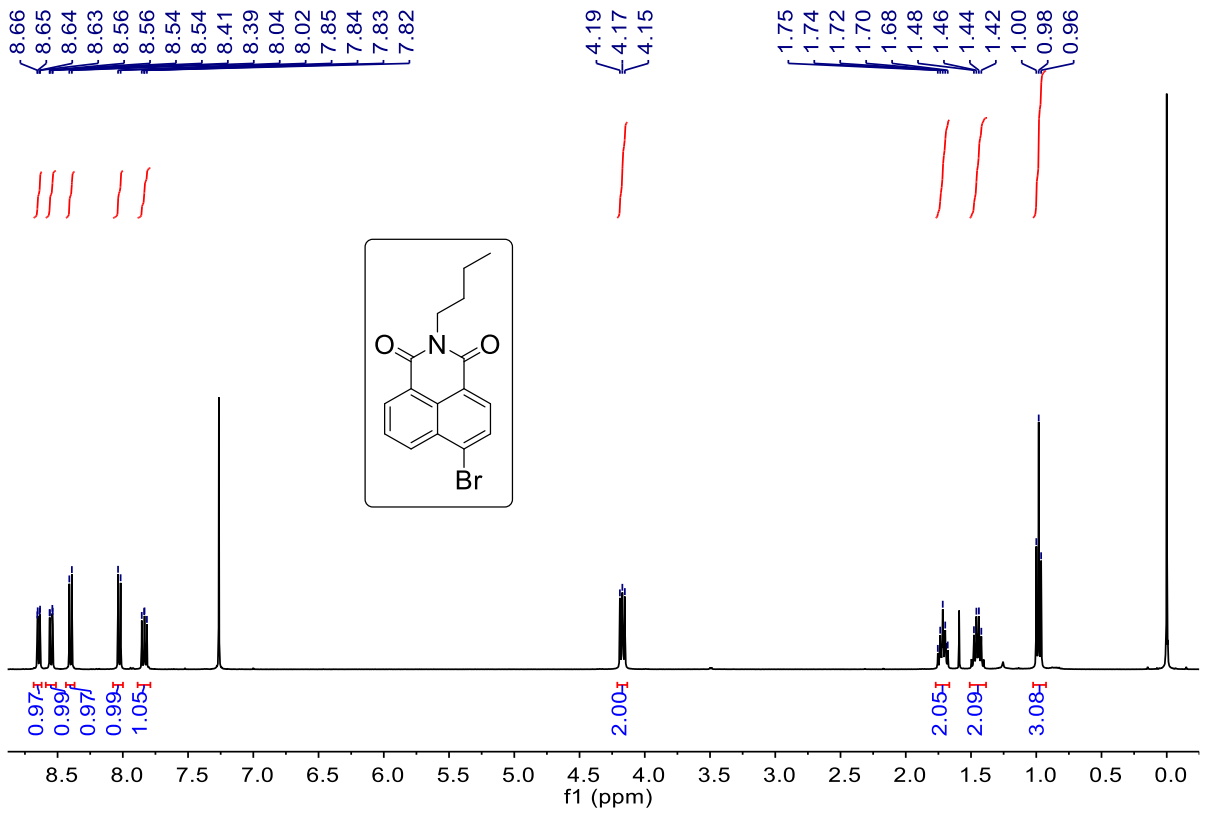

Fig. S4 ^{1}H NMR spectrum of compound **4** in $CDCl_3$ (400 MHz), 25 °C.

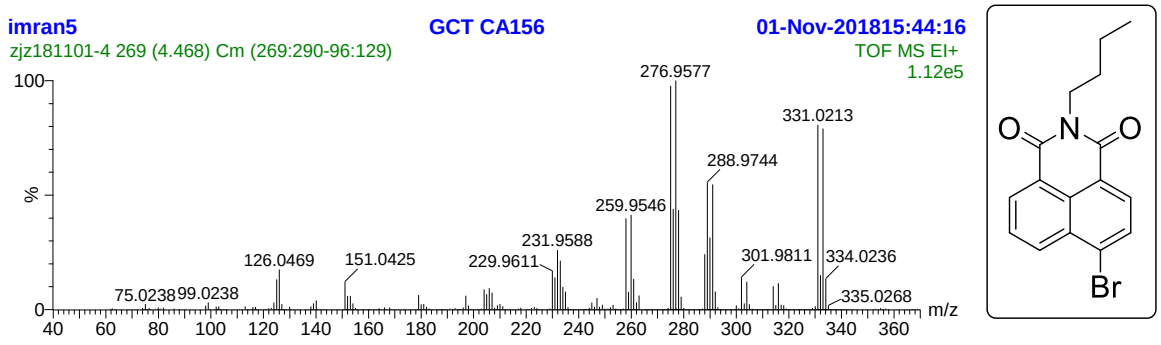

Fig. S5 TOF-MS EI⁺ spectrum of compound **4**.

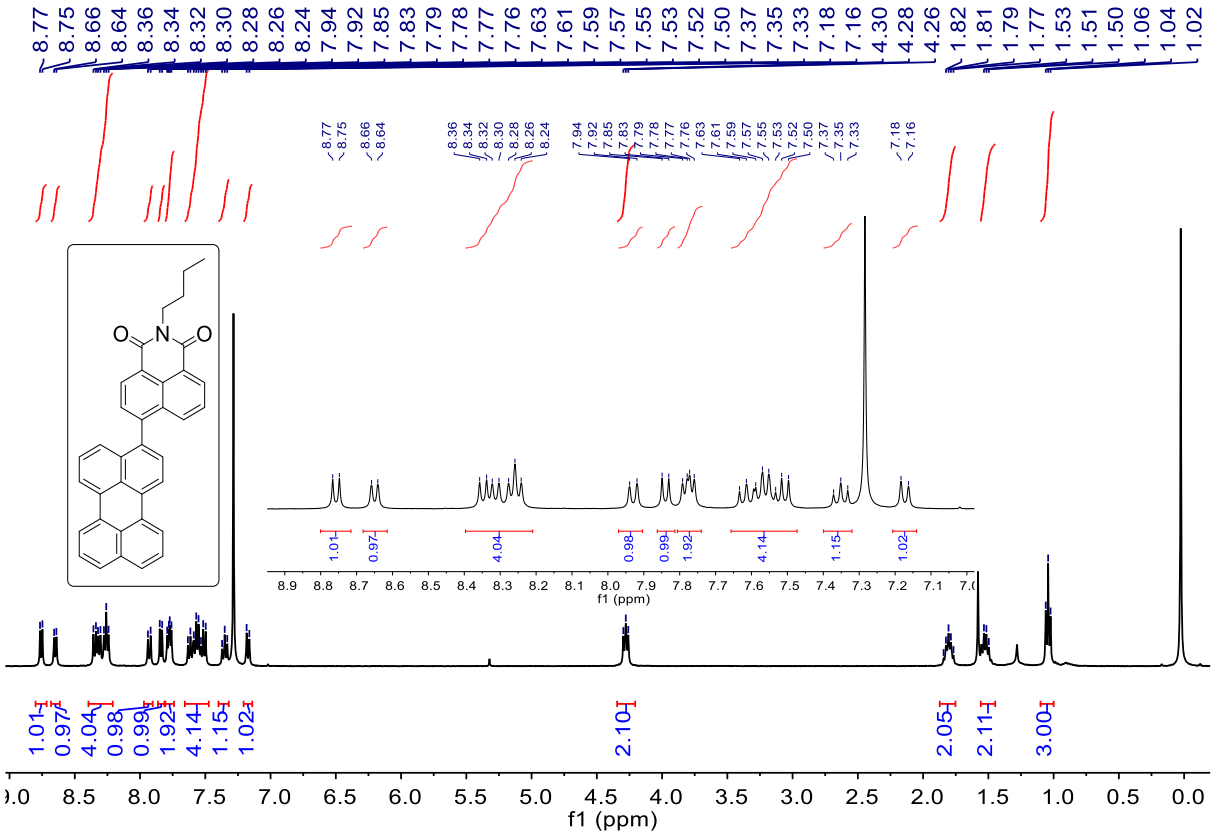

Fig. S6 ^{1}H NMR spectrum of compound **Pery-NI** in $CDCl_3$ (400 MHz), 25 °C.

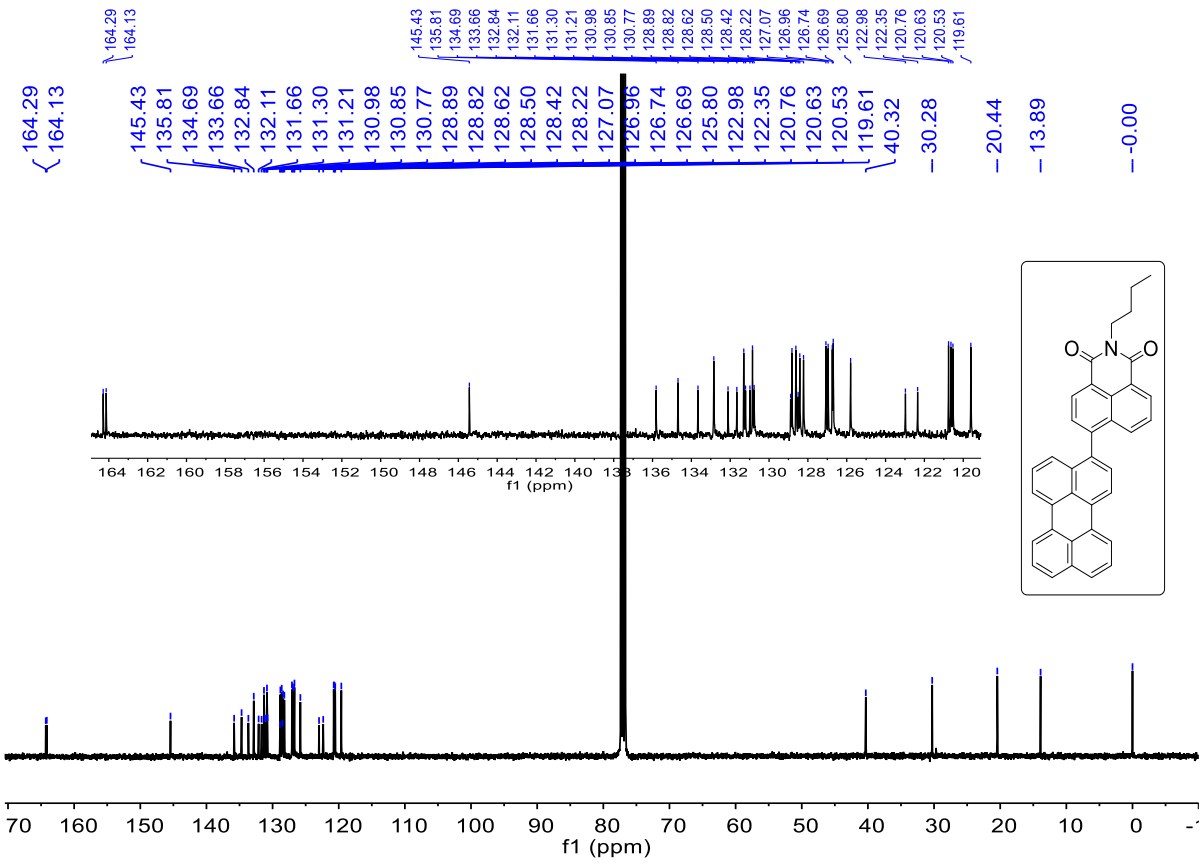

Fig. S7 ^{13}C NMR spectrum of **Pery-NI** in $CDCl_3$ (125 MHz).

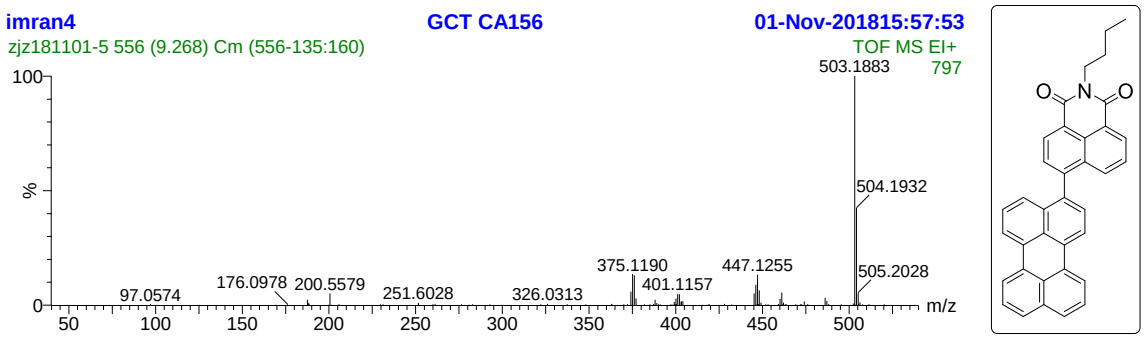

Fig. S8 TOF-MS EI^+ spectrum of **Pery-NI**.

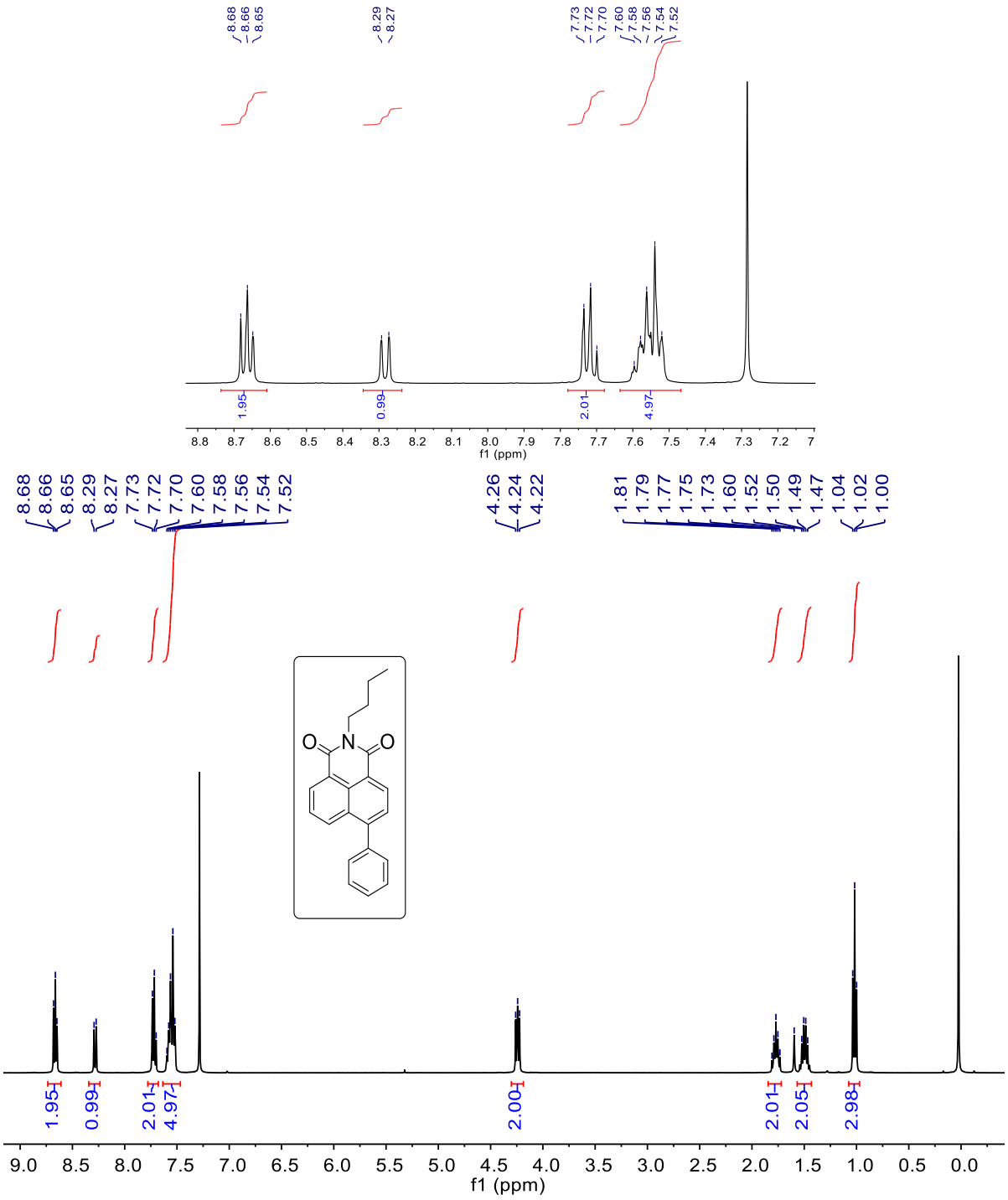

Fig. S9 ^{1}H NMR spectrum of **NI-Ph** in $CDCl_3$ (400 MHz), 25 °C.

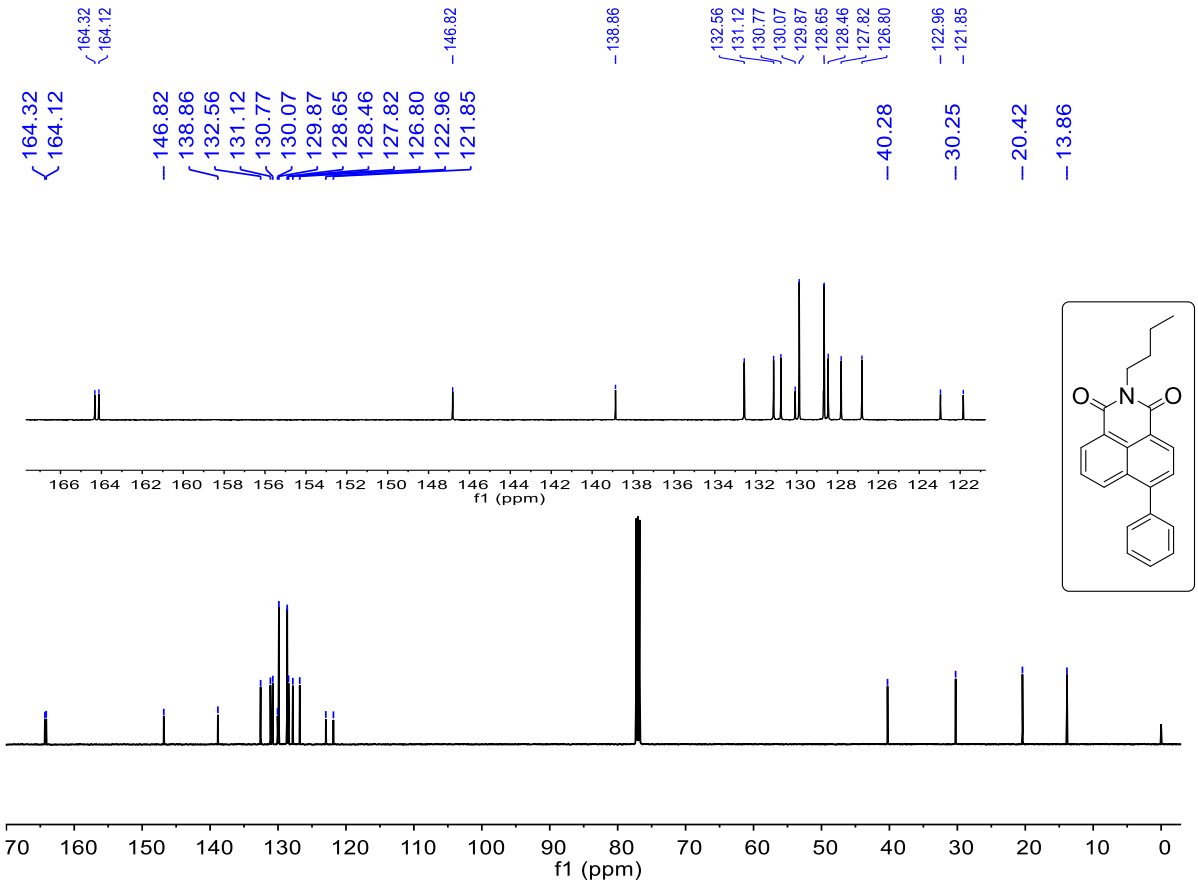

Fig. S10 ^{13}C NMR spectrum of **NI-Ph** in $CDCl_3$ (125 MHz).

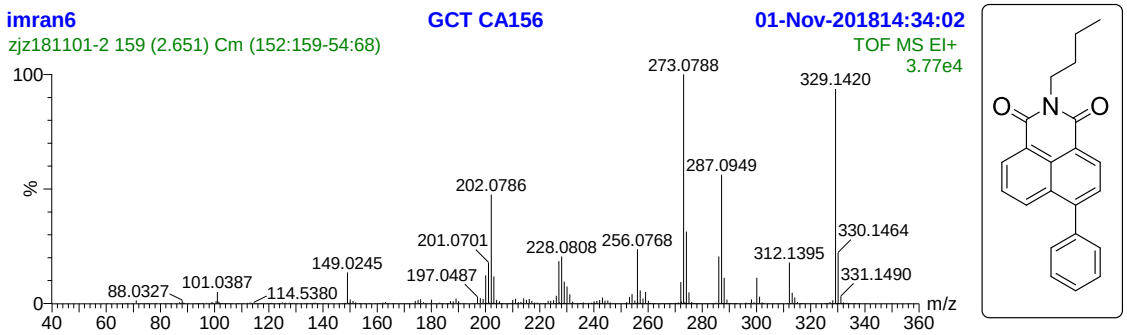

Fig. S11 TOF-MS EI^+ spectrum of **NI-Ph**.

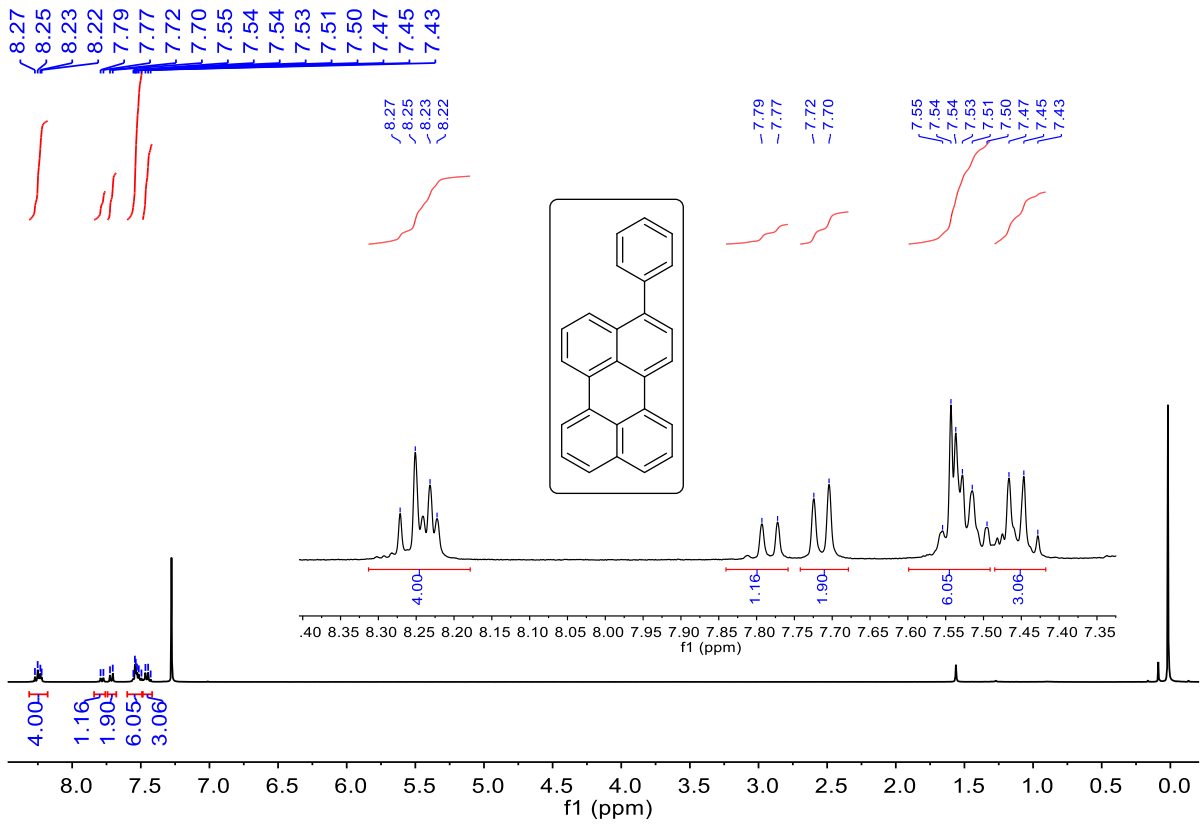

Fig. S12 ^{1}H NMR spectrum of **Pery-Ph** in $CDCl_3$ (400 MHz), 25 °C.

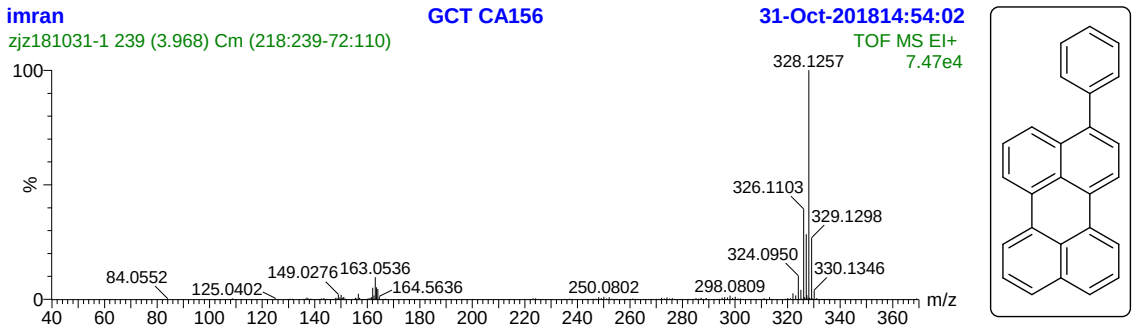

Fig. S13 TOF-MS EI^{+} spectrum of **Pery-Ph**.

3. UV–vis absorption and fluorescence emission spectra

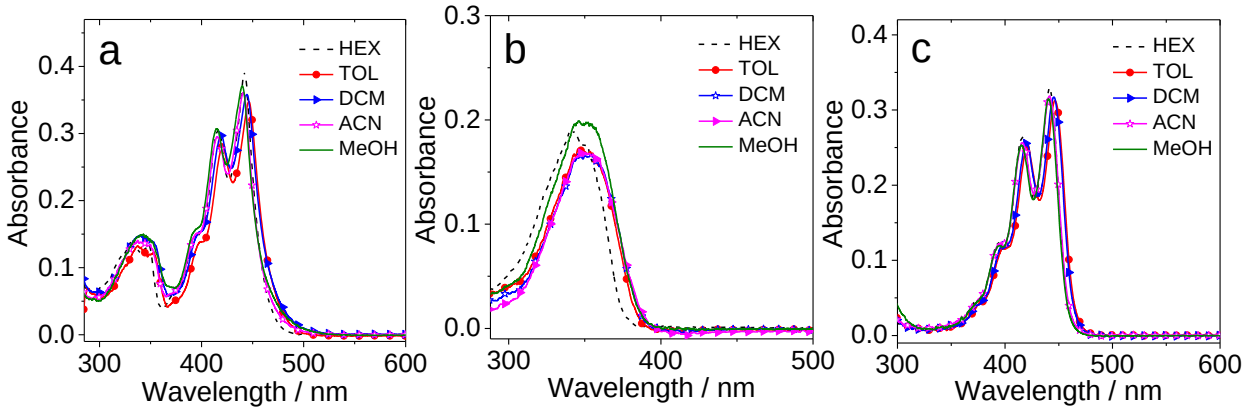

Fig. S14 UV–vis absorption spectra of (a) **Pery-NI**, (b) **NI-Ph** and (c) **Pery-Ph** in different solvents, c = 1.0 × 10^{-5} M, 20 °C.

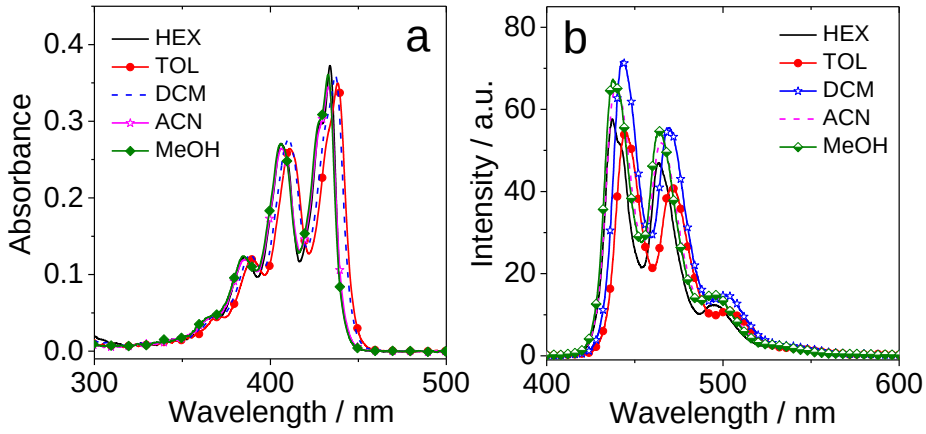

Fig. S15 (a) UV–vis absorption, (b) fluorescence emission spectra of **perylene** in different solvents, c = 1.0 × 10^{-5} M, 20 °C.

4. Fluorescence lifetime spectra

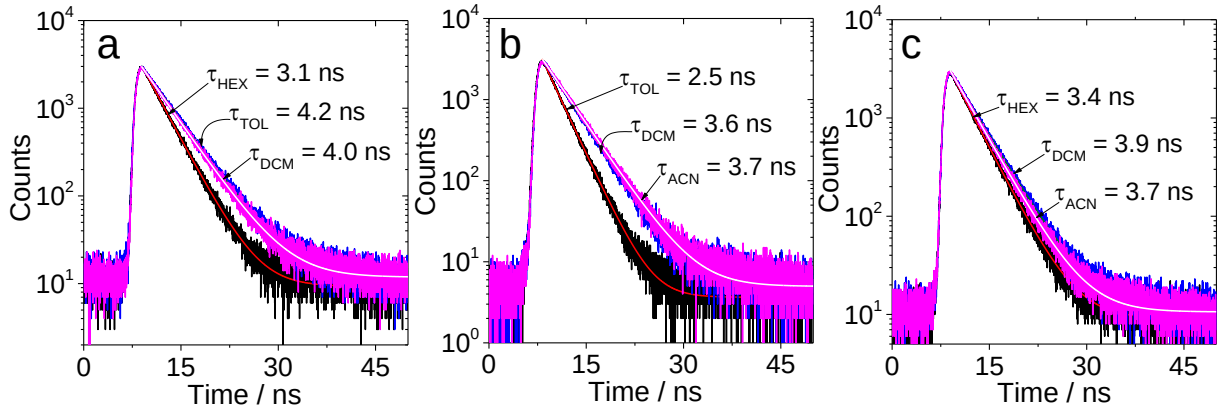

Fig. S16 Fluorescence lifetime decay curves in different solvents. (a) **Pery-NI** at 485 nm in *n*-hexane, at 530 nm in toluene and at 606 nm in DCM, λ_{ex} = 445 nm; (b) **NI-Ph** at 414 nm in toluene, at 420 nm in DCM, at 425 nm in ACN, λ_{ex} = 340 nm; (c) **Pery-Ph** at 454 nm in *n*-hexane, at 461 nm in DCM, at 457 nm in ACN, λ_{ex} = 445 nm. $c = 1.0 \times 10^{-5}$ M. 20 °C.

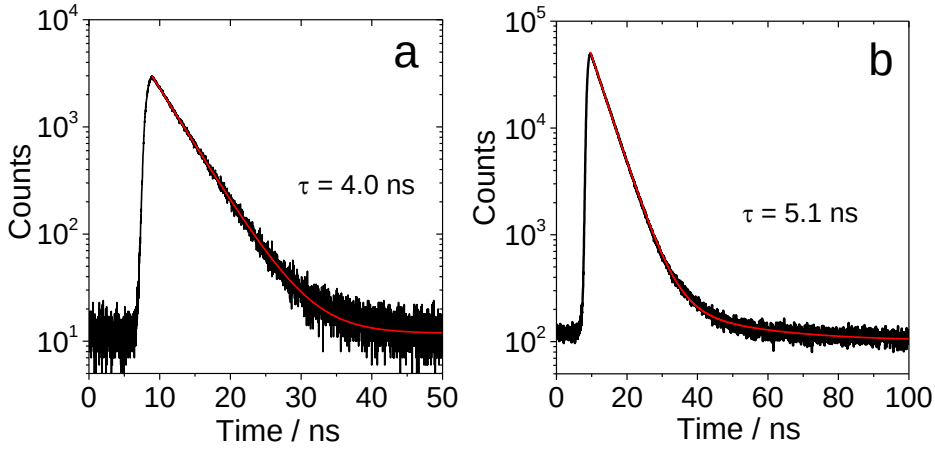

Fig. S17 Fluorescence lifetime decay curves of **Pery-NI** (a) in Air (b) in N_2 at 606 nm in DCM, λ_{ex} = 445 nm, $c = 1.0 \times 10^{-5}$ M. 20 °C.

5. Estimation of Förster Resonance Energy Transfer (FRET) radius (R_0)

The Förster Resonance Energy Transfer (FRET) efficiency (E) and Förster radius (R_0) of the **Pery-NI** dyad upon excitation into the NI moiety, were calculated by using the equation 1 and 2.[5]

$$E = 1 - \frac{F_{DA}}{F_D} \qquad (1)$$

Where 'F_{DA}' is the fluorescence intensity of the donor (NI) in the presence of acceptor, the dyad **(Pery-NI)** and 'F_D' is the fluorescence intensity of the donor (NI) in the absence of acceptor, the (**NI-Ph)**. The absorbance at excitation wavelength is same for both the compounds (λ_{ex} = 323 nm, A = 0.093).

$$E = \frac{1}{1 + \left(\frac{r}{R_0}\right)^6} \qquad (2)$$

Where 'R_0' is the Förster radius, 'E' is FRET efficiency and 'r' is the donor–acceptor distance estimated by the optimize geometry of **Pery-NI**.

The Förster radius (R_0) for the compact donor–acceptor dyad **(Pery-NI)** is calculated as 6.668 Å, and the distance from donor (NI) to acceptor (Pery) is 1.494 Å. As a result, FRET is efficient but if the distance between donor and acceptor is <1 nm, several other modes of energy and/or electron transfer are possible therefore electron transfer to form charge separation state is also efficient in this case as shown in main text Fig. 5c, which imply that FRET and charge separation are competitive processes.

6. Calculation of Gibbs free energy changes of electron transfer

Gibbs free energy changes of photo-induced electron transfer process were calculated using Weller equation 3 and 4.[6, 7] The calculation indicates that the charge separation (electron transfer) is more thermodynamically allowed in polar solvents, which is in agreement with the fluorescence studies.

$$\Delta G^{0}{}_{\mathrm{CS}} = e[E_{OX} - E_{RED}] - E_{00} + \Delta G_{\mathrm{S}} \qquad (3)$$

$$\Delta G_{\mathrm{S}} = -\frac{e^2}{4\pi\varepsilon_{\mathrm{s}}\varepsilon_0 R_{CC}} - \frac{e^2}{8\pi\varepsilon_0}\left(\frac{1}{R_{\mathrm{D}}} + \frac{1}{R_{\mathrm{A}}}\right)\left(\frac{1}{\varepsilon_{REF}} - \frac{1}{\varepsilon_{\mathrm{S}}}\right) \qquad (4)$$

Where ΔG_{CS} is the static Columbic energy, which is described by equation 3. In eq. 3 and 4, e = electronic charge, E_{OX} = half-wave potential of electron-donor unit for one electron oxidation, E_{RED} = half-wave potential of electron-acceptor unit for one electron reduction; E_{00} = approximated energy level with the cross point of normalized UV–vis absorption and fluorescence emission spectra at singlet excited state, ε_{S} = static dielectric constant of the solvent, R_{CC} = center-to-center distance between perylene (electron donor unit) and naphthalimide (electron acceptor unit) determined by DFT optimization of the geometry, R_{CC} [(**Pery-NI**) = 7.69 Å], R_{D}, is the radius of the electron donor, R_{A}, is the radius of the electron acceptor, $\varepsilon_{\mathrm{REF}}$ is the static dielectric constant of the solvent used for the electrochemical studies, ε_0 is the permittivity of free space. Following solvents were used in the calculation of the free energy of electron transfer, toluene (ε_{S} = 2.38), DCM (ε_{S} = 9.1) and ACN (ε_{S} = 37.5)

7. Femtosecond transient absorption spectra

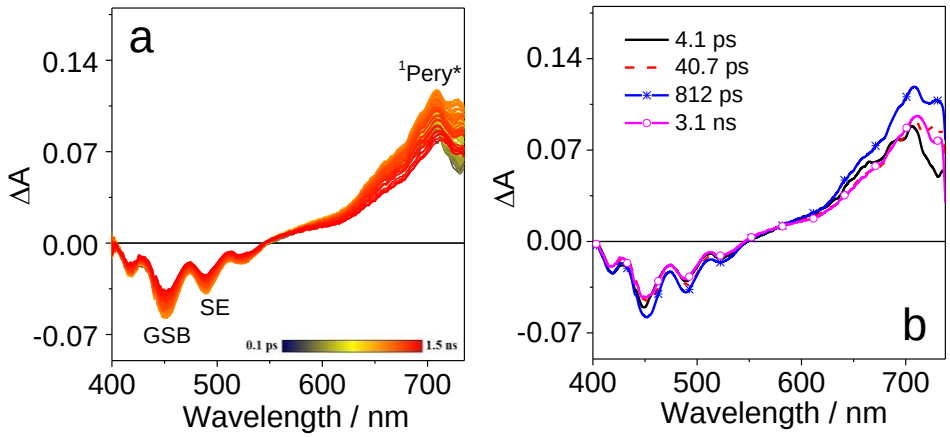

Fig. S18 (a) Femtosecond transient absorption spectra of **Pery-Ph,** in DCM with excitation at 400 nm; (b) Evolution Associated Difference Spectra (EADS) obtained from global analysis.

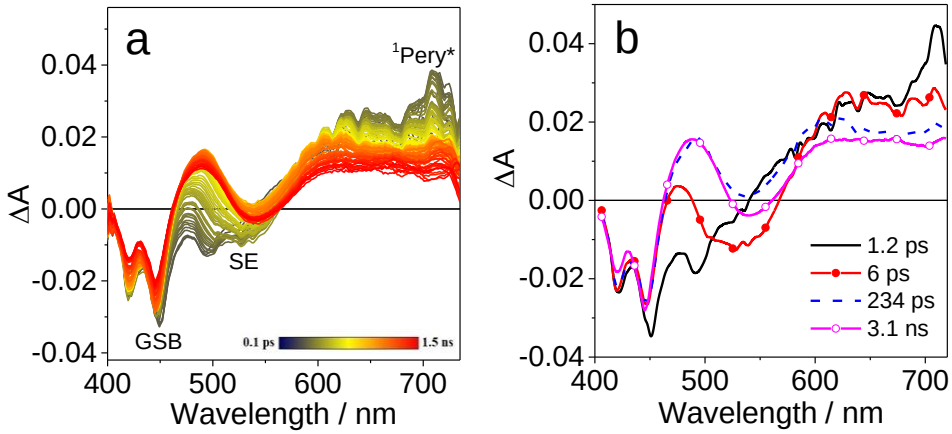

Fig. S19 (a) Femtosecond transient absorption spectra of **Pery-NI,** in toluene with excitation at 400 nm; (b) Evolution Associated Difference Spectra (EADS) obtained from global analysis.

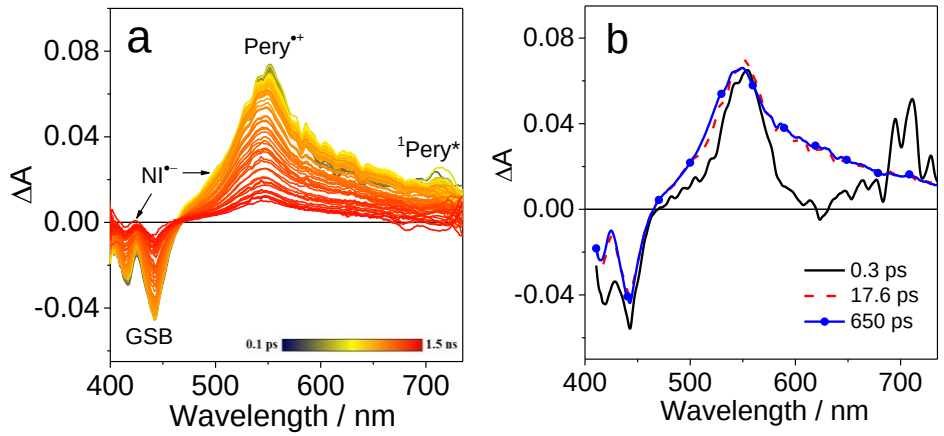

Fig. S20 (a) Femtosecond transient absorption spectra of **Pery-NI,** in ACN with excitation at 400 nm; (b) Evolution Associated Difference Spectra (EADS) obtained from global analysis.

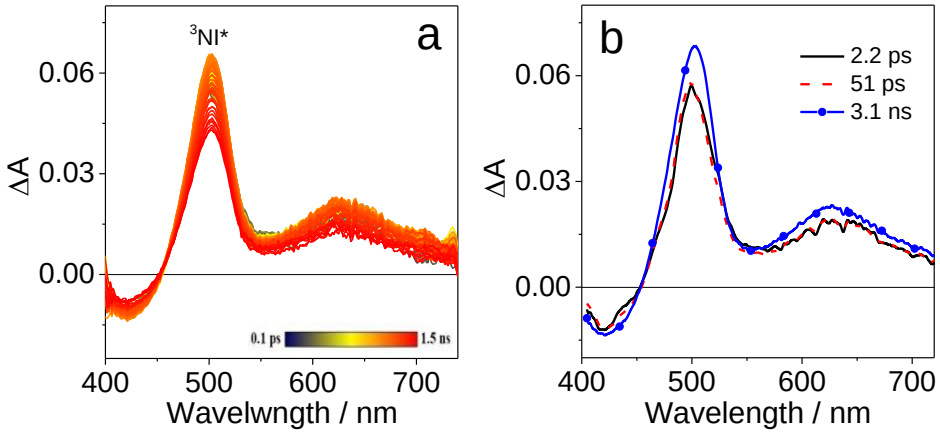

Fig. S21 (a) Femtosecond transient absorption spectra of **NI-Ph,** in DCM with the excitation of 400 nm; (b) Evolution Associated Difference Spectra (EADS) obtained from global analysis.

8. Sub-nanosecond transient absorption spectra

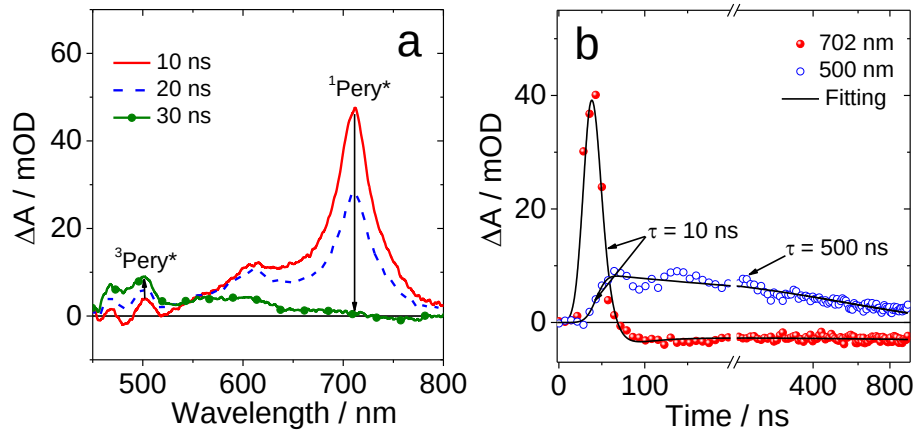

Fig. S22 Subnanosecond transient absorption spectra of Compound **2** (3-bromoperylene) after 350 nm excitation in DCM. (a) Extracted spectra at different time delays and (b) The decay trace at 500 and 702 nm.

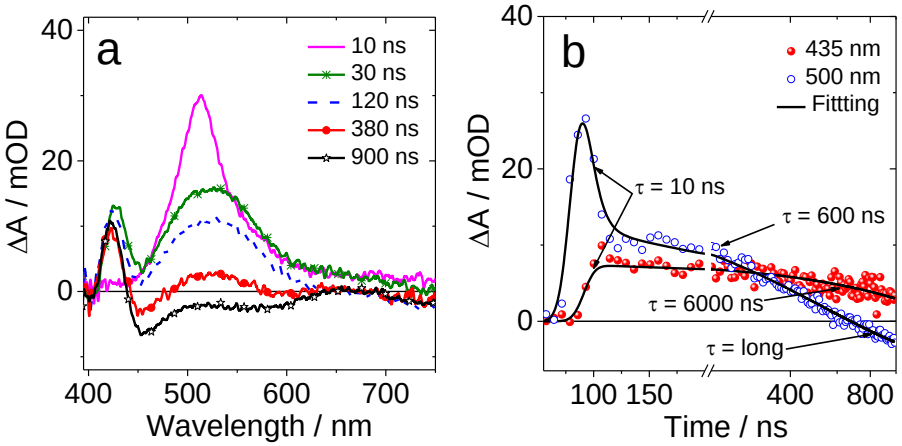

Fig. S23 Subnanosecond transient absorption spectra of **NI-Ph,** after 350 nm excitation in toluene (a) Extracted spectra at different time delays (b) The decay trace at 435 and 500 nm.

9. Nanosecond transient absorption spectra

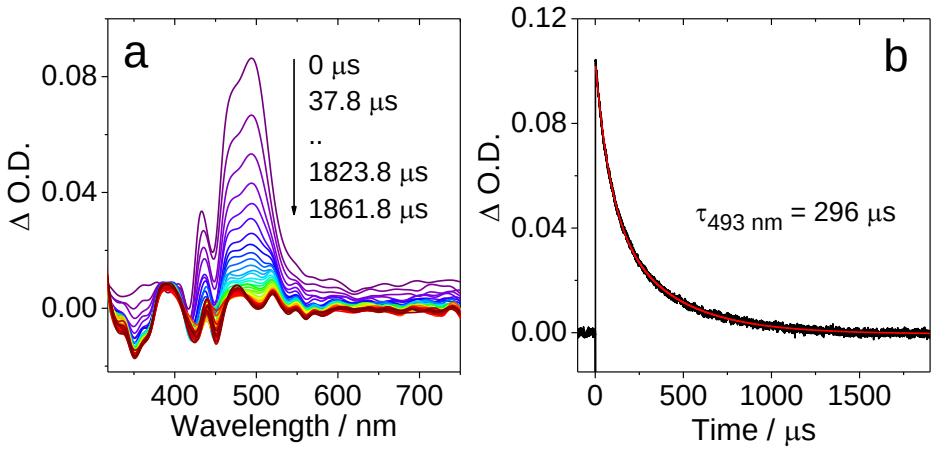

Fig. S24 Nanosecond time-resolved transient absorption spectra of (a) **Pery-NI,** (b) decay trace at 493 nm. λ_{ex} = 445 nm. c = 5.0 × 10^{-6} M. In deaerated toluene. 20 °C.

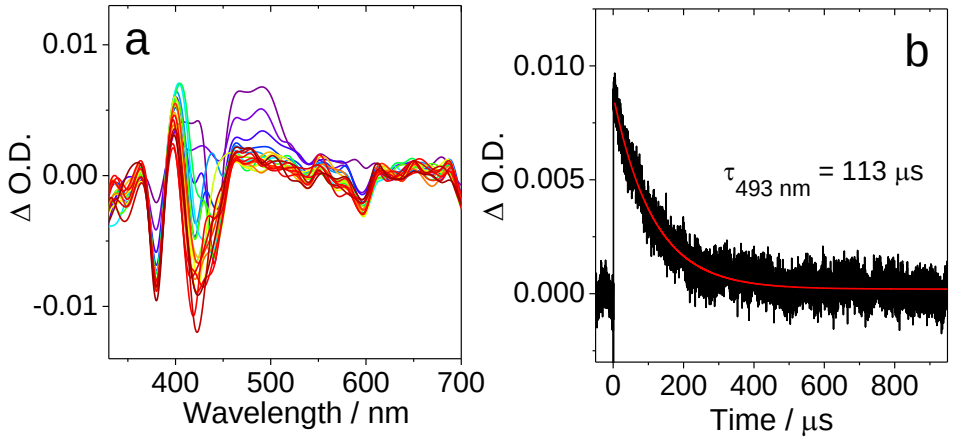

Fig. S25 Nanosecond time-resolved transient absorption spectra of (a) **Pery-NI,** (b) decay trace at 493 nm. λ_{ex} = 445 nm. c = 2.0 × 10^{-5} M. In deaerated ACN. 20 °C. Note; in (a) the spectrum is noisy due to weak signals.

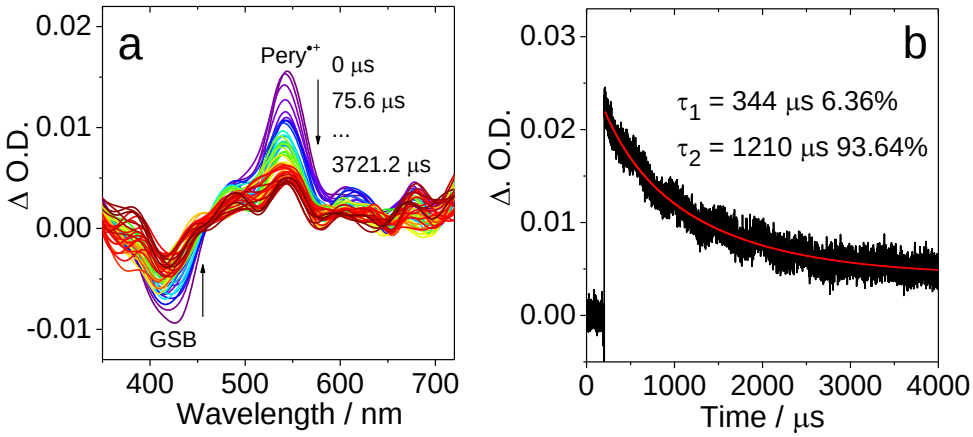

Fig. S26 Nanosecond time-resolved transient absorption spectra of (a) Perylene (b) decay trace at 545 nm. λ_{ex} = 430 nm. c = 1.0 × 10^{-5} M. In aerated DCM. 20 °C.

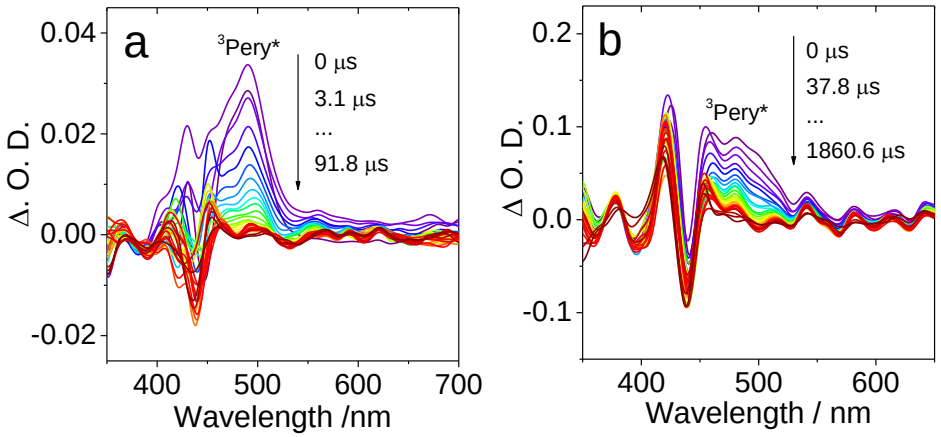

Fig. S27 Nanosecond transient absorption spectra of **Pery-NI,** (a) In deaerated glycerin triacetate and (b) In deaerated triethylene glycol. c = 2.0 × 10^{-5} M. 20 °C.

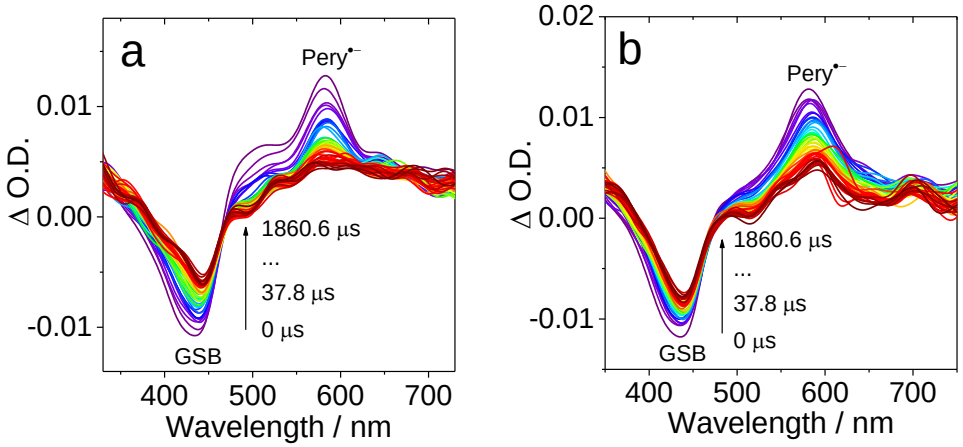

Fig. S28 Nanosecond time-resolved transient absorption spectra of **Pery-Ph**. (a) Under N_2 atmosphere and (b) Under air atmosphere. λ_{ex} = 430 nm. c = 1.0 × 10^{-5} M. In DCM. 20 °C.

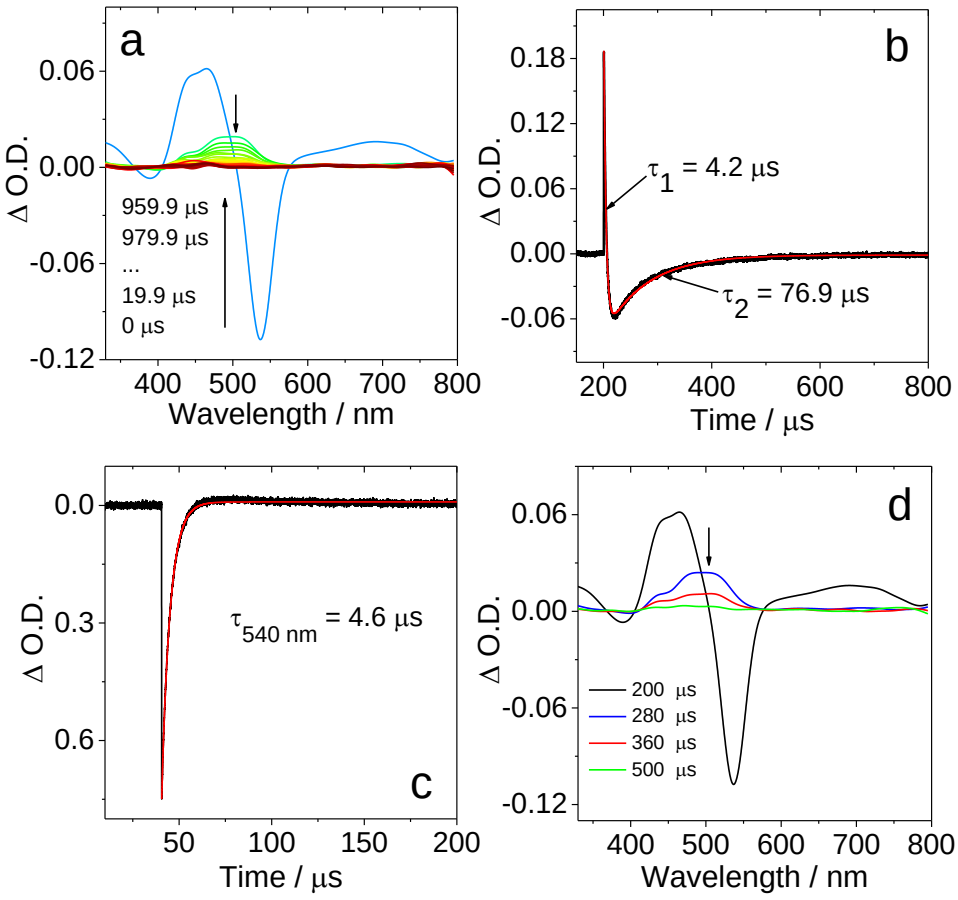

Fig. S29 (a) Intermolecular triplet-triplet energy transfer (TTET) from 2,6-diiodobodipy to **Pery-Ph**, monitored by nanosecond transient absorption spectra of the mixture of triplet energy donor (2,6-diiodobodipy) and acceptor **Pery-Ph**. *c* [2,6-diiodobodipy] = 1.0×10^{-5} M, *c* [**Pery-Ph**] = 4.0×10^{-5} M. (b) Decay trace of the mixture at 490 nm, (c) decay trace of mixture at 540 nm. (d) Transient absorption spectra of the mixture with different delay time. The triplet energy donor 2,6-diiodobodipy was selectively excited at 532 nm with OPO pulsed laser. In deaerated toluene. 20 °C.

10. TREPR spectra

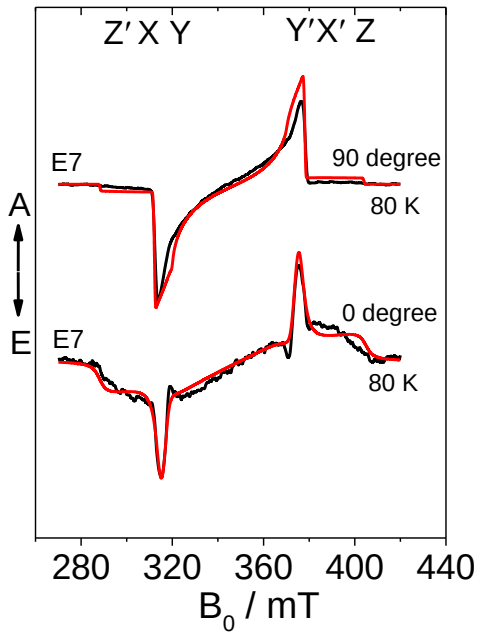

Fig. S30 TREPR spectra of **Pery-NI,** in liquid crystal matrix (E7) recorded with different liquid crystal director against the external magnetic field (0 and 90 degree), following pulsed laser excitation at 445 nm, 10 mJ per pulse. Red lines are computer simulation and black curves are experimental TREPR spectra. A stands for enhanced absorptive positive signal amplitudes, E stands for emissive negative amplitude polarization of the respective transition.

Table S1. Zerofield splitting parameters *D* and *E*, and triplet-state populations sublevels p_1, p_2, p_3 obtained from the simulation of the TREPR spectra with different sample orientation

Compound	Medium	T (K)	$\|D\|$ (MHz)	$\|E\|$ (MHz)	E/D	p_1	p_2	p_3	Order
Pery-NI	E7 ordered 0°	80	1635	35	0.021	0.238	0.000	0.762	0.05
	E7 Ordered 90°	80	1622	74	0.045	0.000	0.342	0.658	0.09

11. DFT computations

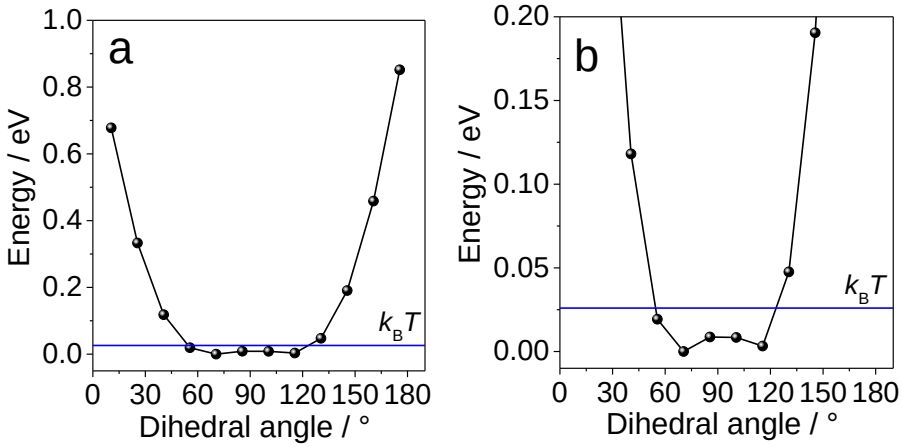

Fig. S31 (a) Calculated ground state (S_0) potential energy curve of **Pery-NI** of the torsion of the linker between the NI and perylene moiety. Blue line shows the thermal (k_BT). (b) Magnified view of (a). Calculations were performed at the (B3LYP/6-31G (d)) level with Gaussian 09W.

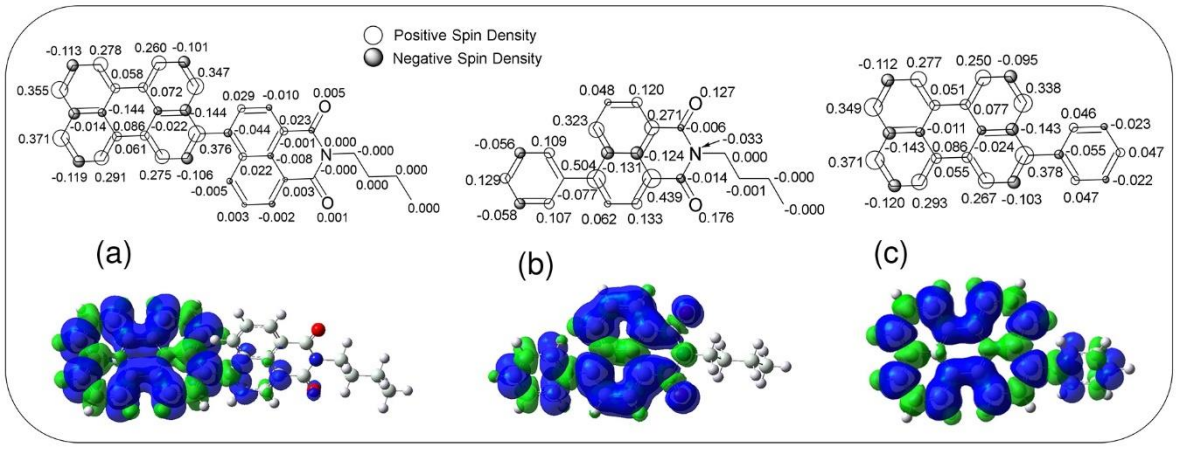

Fig. S32 Spin density distribution of (a) **Pery-NI,** (b) **NI-Ph,** and (c) **Pery-Ph** obtained by B3LYP/6–31G (d) level using Gaussian 09W.

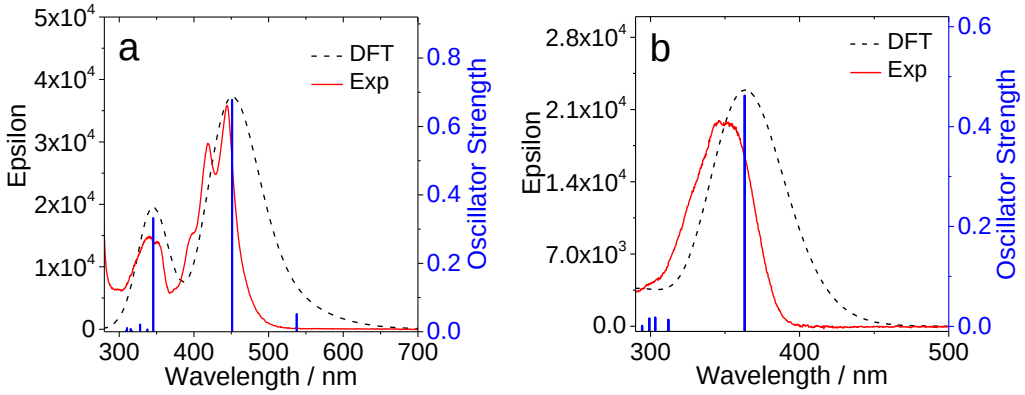

Fig. S33 The comparison of UV−vis results calculated by TD-DFT (B3LYP/6-31G (d)) and experimental data of (a) **Pery-NI**, and (b) **NI-Ph.**

12. TTET/TTA induced delayed fluorescence

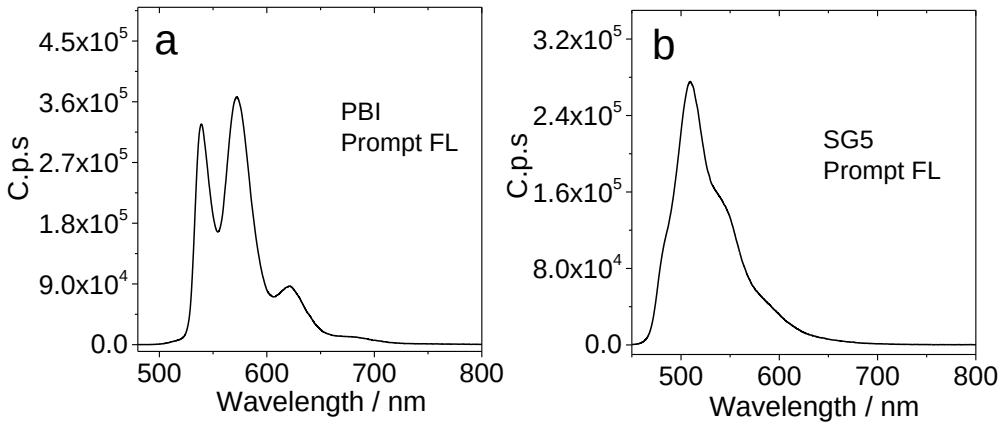

Fig. S34 Fluorescence emission spectra of (a) **PBI**, (λ_{ex} = 445 nm. c = 4.0 × 10^{-5} M) (b) **SG5**, (λ_{ex} = 445 nm. c = 3.0 × 10^{-5} M), in DCM, 20°C.

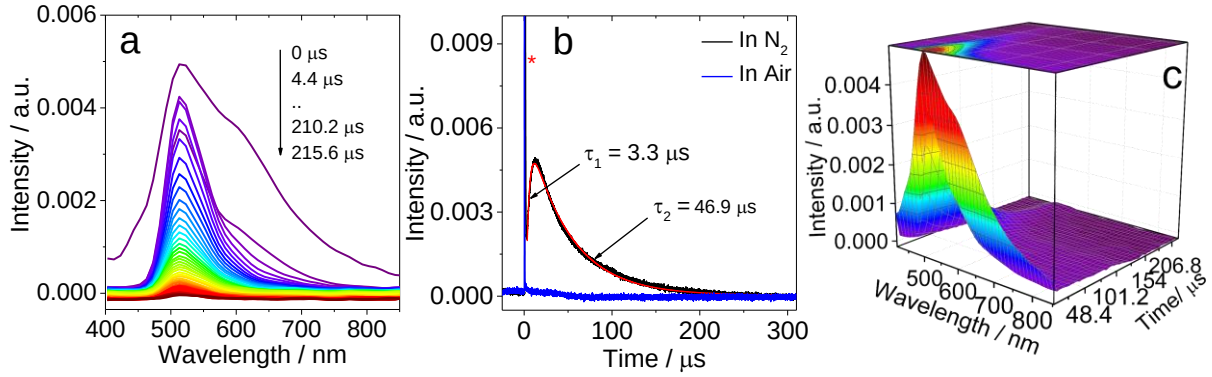

Fig. S35 (a) Delayed fluorescence spectra of the mixture of **Pery-NI** with SG5; (b) decay trace of the fluorescence at 510 nm; (c) 3D spectra of the observed delayed fluorescence. [**Pery-NI**] = 1.0 × 10^{-5} M, [SG5] = 3.0 × 10^{-5} M in DCM. λ_{ex} = 445 nm. The asterisks in (b) indicated the scattered laser.

13. x,y,z coordinates of the optimized geometries

Pery-NI:

Charge = 0; Multiplicity = 1

Symbolic Z−Matrix:

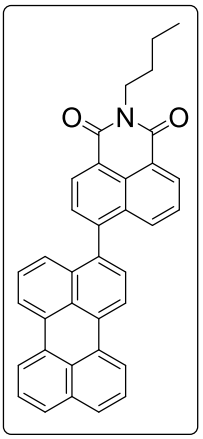

C	6.50146700	-2.02365500	-0.58985800
C	7.87871200	-1.82817900	-0.37772500
C	8.34711800	-0.61448900	0.07051500
C	7.44476400	0.45009700	0.32331600
C	6.03922500	0.25476100	0.10731700
C	5.56977600	-1.01496800	-0.36059200
C	7.91439000	1.70521700	0.78778000
C	7.02942000	2.73025800	1.03257200
C	5.65086900	2.54274400	0.82301700
C	5.13374000	1.33406200	0.36505500
C	3.68877700	1.13300300	0.14021900

C	3.21156800	-0.13879300	-0.31880200
C	4.12281900	-1.21550500	-0.58275900
C	2.76213800	2.14683200	0.35409000
C	1.38749500	1.95110800	0.15069200
C	0.88707000	0.73296200	-0.27016800
C	1.80230700	-0.33829000	-0.53028500
C	1.34704300	-1.59084900	-1.01884900
C	2.23819400	-2.60897100	-1.26950100
C	3.61278900	-2.42324200	-1.04863700
C	-0.58585000	0.58767800	-0.47559600
C	-1.40436900	-0.16398400	0.43186500
C	-2.81171800	-0.24351200	0.19017800
C	-3.38116500	0.42140600	-0.92500700
C	-2.57291700	1.15356000	-1.77498200
C	-1.18637900	1.23352300	-1.54707300
C	-0.88453400	-0.82132600	1.57950500
C	-1.70994900	-1.52956500	2.42996700
C	-3.09344100	-1.61289200	2.17894300
C	-3.64021000	-0.97862900	1.07694000
C	-4.83806200	0.34807700	-1.18556200
C	-5.10108300	-1.07057900	0.83845600
N	-5.60454700	-0.41903400	-0.29671100
O	-5.85280200	-1.68656500	1.58686400
O	-5.36804100	0.92243100	-2.13110200
C	-7.05629000	-0.50631700	-0.54616900
C	-7.84349300	0.61163200	0.14596100
C	-9.35003000	0.50601000	-0.12227800
C	-10.15477600	1.61387700	0.56499400
H	6.17945900	-2.99684300	-0.94160900
H	8.56717300	-2.64590600	-0.57141000
H	9.40898300	-0.45377100	0.23753200
H	8.98106300	1.84019500	0.94679300
H	7.38672100	3.69184900	1.39010000
H	4.99088200	3.37665600	1.03207100
H	3.08445500	3.12492000	0.69112400
H	0.70303600	2.77274200	0.34199300
H	0.28816800	-1.73631100	-1.20141300
H	1.88317800	-3.56451700	-1.64510400
H	4.27651200	-3.25318100	-1.26048800
H	-3.02437200	1.66069200	-2.62110000
H	-0.56786600	1.80575100	-2.23177100
H	0.17852500	-0.75836000	1.78553000
H	-1.29268500	-2.02403700	3.30189100
H	-3.74919800	-2.16679100	2.84222100
H	-7.38131800	-1.48290000	-0.18468600
H	-7.19418900	-0.45832800	-1.62715500

H	-7.47114700	1.58177500	-0.20716500
H	-7.65554900	0.56465100	1.22612800
H	-9.71184300	-0.47448900	0.21787200
H	-9.52961700	0.54095300	-1.20597100
H	-11.22632200	1.51488000	0.35759400
H	-9.83747700	2.60537500	0.21948300
H	-10.02049000	1.58293700	1.65319200

Calculation Type = FREQ

Calculation Method = RB3LYP

Basis Set = 6−31G(d)

Charge = 0

Spin = Singlet

E(RB3LYP) = −1592.2222 a.u.

RMS Gradient Norm = 0.000003 a.u.

Imaginary Freq = 0

Dipole Moment = 5.605510 Debye

Point Group = C1

NI-Ph:

Charge = 0; Multiplicity = 1

Symbolic Z−Matrix:

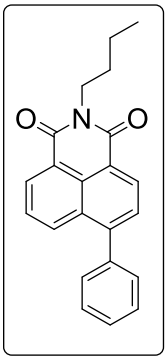

C	-0.23398900	2.76760200	0.19638000
C	1.14360600	2.94060500	0.42706400
C	2.00789700	1.86608400	0.35211300
C	1.53862900	0.56227500	0.03478000
C	0.13146000	0.39064800	-0.16774400
C	-0.73672600	1.51074200	-0.09143400
C	2.39624200	-0.58767100	-0.05243000
C	1.82584100	-1.83377000	-0.28377500
C	0.44208900	-1.99303100	-0.46886400
C	-0.40097500	-0.89736600	-0.42638900
C	-1.85355400	-1.08758900	-0.64379500
C	-2.19524700	1.34982800	-0.30712300
C	3.87451600	-0.49081900	0.09372700
N	-2.65845500	0.05934900	-0.59859900
O	-2.34961900	-2.18918500	-0.85821500

O	-2.97808300	2.29214800	-0.24127700
C	-4.10654700	-0.11277900	-0.82307700
C	-4.87482200	-0.40328400	0.47072300
C	-6.37790800	-0.58023200	0.22115700
C	-7.16152700	-0.87948700	1.50327800
C	4.54570100	-1.31362600	1.01382900
C	5.93460500	-1.26502100	1.13383700
C	6.67900900	-0.39907100	0.33007000
C	6.02500800	0.41725800	-0.59532800
C	4.63569700	0.37387600	-0.71211600
H	-0.92071600	3.60546900	0.25164800
H	1.52695900	3.92602000	0.67384100
H	3.06339800	2.01378700	0.55006300
H	2.47178700	-2.70355100	-0.35393500
H	0.01888900	-2.97292600	-0.66275300
H	-4.22089200	-0.93672100	-1.52883000
H	-4.46652400	0.80843500	-1.28304700
H	-4.71064000	0.42153500	1.17589600
H	-4.46631800	-1.31161500	0.93147400
H	-6.53312200	-1.39414800	-0.50099400
H	-6.77802300	0.32879500	-0.24938500
H	-8.23079000	-1.00244000	1.29688800
H	-7.05288900	-0.06691100	2.23200500
H	-6.80425000	-1.80135300	1.97813900
H	3.97034400	-1.98202200	1.64842500
H	6.43424600	-1.90256900	1.85806400
H	7.76089200	-0.36229100	0.42224600
H	6.59681800	1.08540000	-1.23347200
H	4.13759700	0.99691700	-1.44943800

Calculation Type = FREQ

Calculation Method = RB3LYP

Basis Set = 6−31G(d)

Charge = 0

Spin = Singlet

E(RB3LYP) = −1055.06606318 a.u.

RMS Gradient Norm = 0.00001536 a.u.

Imaginary Freq = 0

Dipole Moment = 5.4266 Debye

Point Group = C1

Pery-Ph

Charge = 0; Multiplicity = 1

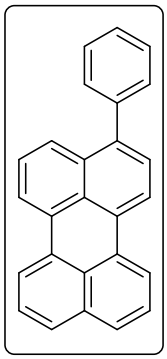

Symbolic Z–Matrix:

C	0.84084900	2.94731700	-0.29399900
C	-0.54135200	2.71104800	-0.22666400
C	-1.05701700	1.42438700	-0.10907000
C	-0.14524200	0.31704500	-0.05598300
C	1.27350500	0.56450200	-0.08441400
C	1.73224000	1.90103900	-0.22317600
C	-0.63292500	-1.02939500	0.00742800
C	0.29547400	-2.06372200	0.03006100
C	1.67618100	-1.82161700	0.02257800
C	2.19150600	-0.53707800	-0.01435200
C	-2.51219200	1.17451800	-0.04720800
C	-2.99163000	-0.17361500	0.01703100
C	-2.08625000	-1.28331800	0.03943600
C	-4.40549200	-0.41800100	0.06219300
C	-4.88439500	-1.75184200	0.11898700
C	-3.99996300	-2.80611200	0.13425500
C	-2.61335900	-2.57081500	0.09682300
C	-3.44284400	2.21014000	-0.04677200
C	-4.82794700	1.96690100	0.00104500
C	-5.30612700	0.67759100	0.05122600
C	3.66986500	-0.35622900	0.02412400
C	4.48607300	-1.02846000	-0.90131800
C	5.87588800	-0.91608200	-0.84660700
C	6.47862100	-0.13160300	0.13866500
C	5.68046600	0.53793000	1.06925000
C	4.29108100	0.42726200	1.01292900
H	1.20316100	3.96519900	-0.40850900
H	-1.20613800	3.56496800	-0.28494800
H	2.79687000	2.09050200	-0.29045300
H	-0.03250000	-3.09587100	0.07141800
H	2.35798700	-2.66564200	0.07666700
H	-5.95724800	-1.92326900	0.15092200
H	-4.36428800	-3.82873300	0.17799500
H	-1.95461400	-3.43133200	0.11580700
H	-3.11342100	3.24210500	-0.08044600
H	-5.51516000	2.80842900	-0.00216300
H	-6.37433300	0.47980000	0.08615600
H	4.02190800	-1.63270300	-1.67606100
H	6.48707600	-1.43947600	-1.57714600
H	7.56076300	-0.04374300	0.18251900

H	6.13999000	1.14257900	1.84668100
H	3.67986500	0.93644500	1.75274100

Calculation Type = FREQ

Calculation Method = RB3LYP

Basis Set = 6−31G(d)

Charge = 0

Spin = Singlet

E(RB3LYP) = −1000.46343670 a.u.

RMS Gradient Norm = 0.00000365 a.u.

Imaginary Freq = 0

Dipole Moment = 0.2318 Debye

Point Group = C1

14. References:

1 M. Imran, A. A. Sukhanov, Z. Wang, A. Karatay, J. Zhao, Z. Mahmood, A. Elmali, V. K. Voronkova, M. Hayvali, Y. H. Xing and S. Weber, *J. Phys. Chem. C*., 2019, **123**, 7010–7024.

2 Y. Avlasevich and K. Müllen, *J. Org. Chem.*, 2007, **72**, 10243–10246.

3 H. zhang, C. Yin, T. Liu, J. Chao, Y. Zhang and F. Huo, *Dyes Pigments.*, 2017, **146**, 344–351.

4 X. Cui, A. Charaf-Eddin, J. Wang, B. Le Guennic, J. Zhao and D. Jacquemin, *J. Org. Chem.*, 2014, **79**, 2038–2048.

5 T. W. J. Gadella, Jr., G. N. M. van der Krogt and T. Bisseling, *Trends in Plant Sci.*, 1999, **4**, 287–291.

6 C. B. KC, G. N. Lim, V. N. Nesterov, P. A. Karr and F. D'Souza, *Chem.–Eur. J.,* 2014, **20**, 17100–17112.

7 R. Ziessel, B. D. Allen, D. B. Rewinska and A. Harriman, *Chem.–Eur. J.*, 2009, **15**, 7382–7393.